

Single-cycle megawatt terahertz pulse generation from a wavelength-scale plasma oscillator driven by ultrashort laser pulses

Hui-Chun Wu, Zheng-Ming Sheng*, and Jie Zhang
*Laboratory of Optical Physics, Institute of Physics,
Chinese Academy of Science, Beijing 100080, China*
(Dated: October 26, 2018)

The tremendous applications of terahertz (THz) spectroscopy and imaging require THz sources in different parameters. We propose a novel scheme to generate single-cycle powerful THz pulses by ultrashort intense laser pulses incident obliquely on a tenuous plasma slab of few THz wavelengths in thickness. This is made possible by driving a large amplitude electron plasma wave in the plasma slab, thus producing a net transient current at the plasma surfaces. Theory and simulations show that such a THz source is capable of providing megawatt power and field strength of MV/cm, which may open up new horizons for nonlinear THz science and applications.

PACS numbers: 42.65.Re, 42.72.Ai, 52.25.Os, 52.59.Ye

Terahertz spectroscopy can probe the spectral properties of molecules in a previously inaccessible electromagnetic spectrum [1]. Its applications include the characterization of semiconductors [2] and high-temperature superconductors [3], T-ray imaging of biomedical tissues [4], cellular structures [5] and dielectric substances [6], and the manipulation of bound atoms [7]. Most applications are based on the techniques of THz time-domain spectroscopy (THz-TDS) [1], where typically coherent broadband THz pulses in the 2-5 THz frequency bandwidth are employed. Most broadband pulsed THz sources are based on the excitation of different materials with ultrashort laser pulses [1], such as through photoconduction or optical rectification, but the output power is limited by the damage threshold of the optical materials used.

So far, there have been no development in the nonlinear regime due to the lack of sufficiently high power THz sources [1]. To address this problem a few efforts have been made using ultrashort electron bunches produced by lasers or accelerators through the mechanisms of transition radiation and/or synchrotron radiation [8].

Recently, by four-wave mixing in air with a laser intensity of $\sim 10^{14}$ W/cm², single-cycle THz pulses with a field strength greater than kV/cm can be produced [9], after the laser field-ionization and plasma generation threshold is surpassed. Whether this kind of THz emission will saturate for light intensities $> 10^{15}$ W/cm² is an open question.

For light intensities $\gg 10^{14}$ W/cm², the leading part of the laser pulse can completely ionize the material and the interaction process becomes a pure laser-plasma interaction. Plasma has no thermal damage threshold and can sustain extremely intense light. The peak intensity of lasers today can be as high as 10^{20} W/cm² and in the future is expected to reach 10^{23} W/cm² [10]. Exploring new THz emission mechanisms in the context of intense

laser plasma interactions may produce higher power THz sources. It has been shown that laser wakefields (electron plasma waves driven by the ponderomotive force of a laser pulse) in inhomogeneous plasmas can radiate high-efficiency THz waves at high power through linear mode conversion [11, 12]. The THz pulses produced in this way are generally in multi-cycles and have a negative frequency chirp.

The present work introduces a new THz emission mechanism in laser plasma interaction, which can directly generate a single-cycle THz pulse with a field strength comparable with our earlier proposal [11, 12]. In addition to the above applications, the single-cycle pulse has special implications for THz propagation physics and seismic surveys [13]. In the one-dimensional (1D) case, an electron plasma wave [14] in a uniform plasma is described by $\delta n = \delta n_p \exp[i(k_p x - \omega_p t)]$, where δn_p is the density perturbation amplitude, $\omega_p = \sqrt{ne^2/m\epsilon_0}$ is the plasma frequency of the background plasma of density n , $-e$ and m are the electron charge and mass respectively, and $k_p = \omega_p/c = 2\pi/\lambda_p$, where λ_p is the plasma wavelength. This infinite plasma wave can never emit electromagnetic waves at frequency ω_p , since its displacement current ($\epsilon_0 \partial E / \partial t$) exactly compensates the plasma current ($-env$). However, for a finite plasma wave of length $L \sim \lambda_p$, there could be some electromagnetic radiation. Firstly, for such a few-wavelength plasma oscillator, its displacement and plasma currents cannot completely counteract each other, in particular near the plasma boundaries. Secondly, since the plasma skin depth of the radiation at frequency ω_p is k_p^{-1} , which is comparable to the plasma length L , the radiation can tunnel through the plasma into vacuum. Figure 1(a) is a schematic of this THz wave emission mechanism.

In the following we give a theoretical analysis of this THz emission mechanism. For the interaction geometry shown in Fig. 1(a), by Lorentz transformations we transform all the physical quantities from the laboratory frame to a moving frame of velocity $c \sin \theta \mathbf{e}_y$, where \mathbf{e}_y is the unit vector along the y direction. An electromagnetic wave with $\omega^L = \omega'$, $\mathbf{k}^L = (\pm k' \cos \theta, k' \sin \theta, 0)$

*e-mail: zmsheng@aphy.iphy.ac.cn

in the laboratory frame becomes $\omega^M = \omega' \cos \theta$, $\mathbf{k}^M = (\pm k' \cos \theta, 0, 0)$ in the moving frame, wherein all the electromagnetic waves propagate along the $\pm x$ directions, i.e. THz emission in the laboratory frame must be in the specular reflection and laser transmission directions. Plasma (electrons and ions) in the moving frame streams along $-\mathbf{e}_y$, with a relativistic factor $\gamma^M = 1/\cos \theta$. Following Ref. [15] and using the quasi-static approximation [16], we obtain the coupled equations (in SI units)

$$\left(\frac{\partial^2}{\partial x^2} - \frac{1}{c^2} \frac{\partial^2}{\partial t^2} \right) \mathbf{a}_T = \frac{\omega_p^2}{c^2} \mathbf{s}(x, t), \quad (1)$$

$$\frac{\partial^2 \phi}{\partial x^2} = \frac{\omega_p^2}{c^2} \delta n, \quad (2)$$

$$\delta n = \frac{1}{2 \cos \theta} \left[\frac{1 + (\mathbf{a}_L - \mathbf{e}_y \tan \theta)^2}{(1/\cos \theta + \phi)} - 1 \right], \quad (3)$$

where $\mathbf{s}(x, t) = -\delta n \tan \theta \mathbf{e}_y / \gamma$ is the THz radiation source, \mathbf{a}_T and \mathbf{a}_L are the respective vector potentials of the THz wave and incident laser normalized by mc/e , ϕ is the scalar potential of the driven plasma wave normalized by mc^2/e , δn is the density perturbation of the plasma wave normalized by the initial plasma density n , $\gamma = \sqrt{1 + (\mathbf{a}_L - \tan \theta \mathbf{e}_y)^2 + p_x^2}$ is the electron relativistic factor, and p_x is the electron longitudinal momentum normalized by mc .

The generation of the THz radiation is determined by Eq. (1), from which the electric field in the laboratory frame is found to be [15]

$$\mathbf{e}_T^L(x, t) = \frac{\omega_p}{2\omega \cos \theta} \int_0^L \frac{dx'}{k_p^{-1}} \mathbf{s}(x', t - |x - x'|/c), \quad (4)$$

where L is the plasma length, ω the laser frequency, and normalization with respect to $m\omega c/e$ has been performed. Equation (4) shows that the THz emission is always p -polarized. In the weakly relativistic case $\phi \ll 1$, Eqs. (2) and (3) lead to $\delta n \propto a_L^2 \cos \theta$. In the THz emission process, we assume $\gamma \simeq \gamma^M$. Substituting these into Eq. (4) we obtain

$$e_T^L \propto n^{1/2} a_L^2 \sin \theta \quad (5)$$

for $L \sim \lambda_p$. From Eq. (5) we can see that there is no THz emission for normal incidence ($\theta = 0$), since there is no transverse electric field component.

To test our proposal and the scaling rule in Eq. (5) we conduct a series of 1D particle-in-cell (PIC) simulations. Taking into account the oblique incidence of the laser beam, our 1D-PIC code adopts a moving frame as discussed above [15] and outputs all physics quantities in the laboratory frame. The initial plasma density is taken to be $n = 0.0001 n_c$, where $n_c = m\epsilon_0 \omega^2 / e^2 = 1.1 \times 10^{21} (\mu\text{m}/\lambda)^2 \text{ cm}^{-3}$ is the critical density for the laser pulse of wavelength λ in vacuum. For $\lambda = 1 \mu\text{m}$,

$n = 1.1 \times 10^{17} \text{ cm}^{-3}$. The corresponding plasma frequency is $\omega_p / 2\pi = 2.98 \text{ THz}$, which represents the central frequency of the THz emission. The plasma wavelength is $\lambda_p = \sqrt{n_c/n} \lambda = 100\lambda$. The incident laser pulse has a sine-square profile $a_L = eE_L / m\omega c = a_0 \sin^2[\pi(x-ct)/d_L]$ for $0 \leq x - ct \leq d_L$, where d_L is the laser pulse duration. Here a_0 is related to the peak laser intensity through $I = a_0^2 \cdot 1.37 \times 10^{18} (\mu\text{m}/\lambda)^2 \text{ W/cm}^2$. The relativistic intensity threshold is reached at $a_0 = 1$. The laser pulse enters the left boundary of the simulation box with s polarization in order to distinguish it easily from the p -polarized THz emission from the wakefield. For the sine-square laser pulse, the excited wakefield amplitude is maximum when $d_L \approx \lambda_p$ [12]. The simulation results also confirm that the THz emission is strongest for $d_L = \lambda_p$, thus we always set $d_L = \lambda_p$ in the following.

Defining fields $F_{\pm} = (E_y \pm cB_z)/2$ in the moving frame, we see that F_+ and F_- represent the forward and backward p -polarized electromagnetic waves, respectively. Tracing F_+ and F_- at the right and left boundaries of the simulation box, we can obtain the temporal profile of the radiated THz pulses in the reflection and transmission directions. Figure 1(b) shows the peak field strengths $|F_{\pm}|_{\text{max}}$ of the THz pulses as a function of the plasma length L . The laser pulse parameters are $a_0 = 0.5$, $d_L = 100\lambda$ and $\theta = 45^\circ$. The incident laser intensity is about $3.4 \times 10^{17} \text{ W/cm}^2$ ($\lambda = 1 \mu\text{m}$). We find that the plasma length L should be within $[0.25\lambda_p, 2.7\lambda_p]$ for intense THz pulses to be generated. When $L \geq 3\lambda_p$, the THz pulse amplitude decreases dramatically.

We also find that the radiated THz pulse is single-cycle. Figures 1(c) and 1(d) show the time evolution of field components E_x and B_z in the x space for $L = 100\lambda$. The field E_x in Fig. 1(c) includes the longitudinal field of the wakefield and the electric field of the p -polarized THz emission. The wakefield is completely localized in the plasma region, while the electric field of the THz wave is mainly outside the plasma slab. In Fig. 1(d) B_z is the pure magnetic field of the THz wave. It is obvious that two single-cycle THz pulses are radiated from the plasma region. Due to the propagation delay of the laser pulse, the pulse in the backward (reflection) direction is generated earlier than that in the forward (transmission) direction. For the specific laser wavelength $\lambda = 1 \mu\text{m}$ in Fig. 1(d), the field strength is found to be above 10 MV/cm. When $L \geq 3\lambda_p$, the THz pulse is no longer single-cycle.

Figures 2(a) and 2(b) illustrate the temporal profiles of the THz pulses shown in Figs. 1(c) and 2(d) together with two other incident angles of 30° and 60° . The shape of the transmitted THz wave F_+ is the same as that of the reflected F_- . For $\theta = 30^\circ$, the THz pulses have two cycles. Single-cycle THz emission is produced when $\theta \geq 45^\circ$. With increasing incident angle, the number of cycles included in the THz pulse decreases. Figure 2(c) displays the power spectra of the THz pulses F_- . The central frequency is at 3 THz ($\lambda = 1 \mu\text{m}$). The spectrum width increases with the incident angle, because of

the shorter THz duration for the larger θ . The bandwidths approach 3-6 THz, meeting the requirements for the THz-TDS system. Figure 2(d) shows that the peak field strengths $|F_{\pm}|_{\max}$ are proportional to $\sin\theta$, which agrees with Eq. (5). There is no THz emissions for $\theta = 0$.

Figures 3(a) and 3(b) show that the THz field strength is proportional to both the laser intensity, i.e. a_L^2 , and the square root of the plasma density n . At lower intensities of 10^{14} - 10^{15} W/cm², the THz field strength is several tens of kV/cm, comparable to that generated through four-wave mixing in air [9] under the same intensities.

The above 1D theoretical analysis and 1D-PIC simulations are valid as long as the laser spot size is large compared with the plasma wavelength. For a laser beam with a Gaussian profile $\exp(-r^2/w_L^2)$ in transverse space, the 1D model applies for $w_L \gg \lambda_p$. It is easily understood that, for $w_L < \lambda_p$, the radiation source size is smaller than the radiated wavelength, so that the generated THz wave will diffract dramatically. In order to have collimated THz emission, $w_L \gg \lambda_p$ should be maintained.

To illustrate the multi-dimensional properties of the THz emission, Fig. 4 shows the THz emission in a 2D-PIC simulation. It is found that there are indeed two single-cycle THz pulses in the reflection and transmission directions. For $\lambda = 1 \mu\text{m}$, the THz field strength is 42 MV/cm, i.e. an intensity of 2.5×10^{12} W/cm². Since the radiation radius is about $30\mu\text{m}$, this is equivalent to a peak power of 70 MW.

A uniform plasma slab several tens of microns long can be readily formed from the gas jet targets commonly used in high-harmonic generation experiments [17]. Meanwhile, our numerical simulations show that THz pulses emitted from a nonuniform plasma with a trapezoid density profile are similar to those from a uniform plasma slab, provided that the ascending and descending parts of the trapezoid are also at the THz wavelength scale. This suggests that the density homogeneity of the plasma slab is not necessary.

To conclude, we have presented a method for producing single-cycle high power THz radiation from wavelength-scale plasma oscillators ($L \sim \lambda_p$). It is emitted by the transient net currents induced at the plasma surfaces while building-up the plasma oscillators. This mechanism together with that for THz emission by linear mode conversion in inhomogeneous plasmas ($L \gg \lambda_p$) [11, 12] provide a complete picture for interpreting the early experimental observation of THz emission in intense laser plasma interaction [18].

Acknowledgments

Authors are grateful to Prof. Ling-An Wu for careful reading of the manuscript and improving the text, and Dr. Yu Cang for useful discussions. This work was supported by the China NNSF (Grants No. 10335020,

10425416, 10390160, 10476033, and 10576035), the National High-Tech ICF Committee in China, and the Knowledge Innovation Program, CAS.

-
- [1] B. Ferguson and X.-C. Zhang, *Nat. Mater.* **1**, 26 (2002).
 [2] D. Grischkowsky *et al.*, *J. Opt. Soc. Am. B* **7**, 2006 (1990).
 [3] R. A. Kaindl *et al.*, *Phys. Rev. Lett.* **88**, 027003 (2002).
 [4] T. Löffler *et al.*, *Optics Express* **9**, 616 (2001).
 [5] O. Mitrofanov *et al.*, *IEEE J. Sel. Top. Quantum. Electron.* **7**, 600 (2001).
 [6] B. Ferguson *et al.*, *Opt. Lett.* **27**, 1312 (2002).
 [7] B. E. Cole *et al.*, *Nature* **410**, 60 (2001).
 [8] G. L. Carr *et al.*, *Nature* **420**, 153 (2002); M. Abo-Bakr *et al.*, *Phys. Rev. Lett.* **90**, 094801 (2003); W. P. Leemans, *et al.*, *ibid.* **91**, 074802 (2003).
 [9] D. J. Cook and R. M. Hochstrasser, *Opt. Lett.* **25**, 1210 (2000); M. Kress *et al.*, *ibid.* **29**, 1120 (2004); T. Bartel *et al.*, *ibid.* **30**, 2805 (2005); X. Xie, J. Dai, and X.-C. Zhang, *Phys. Rev. Lett.* **96**, 075005 (2006).
 [10] G. A. Mourou *et al.*, *Rev. Mod. Phys.* **78**, 309 (2006).
 [11] Z.-M. Sheng, K. Mima, J. Zhang, and H. Sanuki, *Phys. Rev. Lett.* **94**, 095003 (2005).
 [12] Z.-M. Sheng, K. Mima, and J. Zhang, *Phys. Plasmas* **12**, 123103 (2005).
 [13] T. D. Dorney *et al.*, *Geophysics* **68**, 308 (2003).
 [14] E. Esarey *et al.*, *IEEE Trans. Plasma Sci.* PS-24, 252 (1996).
 [15] R. Lichters, J. Meyer-ter-Vehn, and A. Pukhov, *Phys. Plasmas* **3**, 3425 (1996).
 [16] P. Sprangle *et al.*, *Phys. Rev. A* **41**, 4463 (1990).
 [17] Ch. Spielmann *et al.*, *Science* **278**, 661 (1997).
 [18] H. Hamster *et al.*, *Phys. Rev. Lett.* **71**, 2725 (1993).

Figure Captions

FIG. 1 (color online). (a) Schematic of THz emission from a few-wavelength long plasma oscillator excited by a laser pulse obliquely incident on a uniform plasma slab. The plasma length is $L \sim \lambda_p$ and θ is the laser incident angle. THz waves are radiated in the specular reflection and laser transmission directions, similar to the optical rectification scheme. (b) The peak field strengths $|F_{\pm}|_{\max}$ of the radiated THz pulses as a function of the plasma length L . The plasma is of density $n = 0.0001n_c$. The laser pulse parameters are $a_0 = 0.5$, $d_L = 100\lambda$ and

$\theta = 45^\circ$. Spatial-temporal plots of (c) the electric field E_x and (d) the pure THz magnetic field B_z for the plasma length $L = 100\lambda$ (located in $100\lambda \leq x \leq 200\lambda$). The vertical dashed lines represent the plasma boundaries. The dashed arrow line marks the laser propagation trajectory. Other parameters are the same as in (b).

FIG. 2 (color online). Temporal profile, frequency spectrum and field amplitude of the THz emission. (a) Temporal profiles of the THz waves F_+ for incident angles of $\theta = 30^\circ$, 45° and 60° . (b) Temporal profiles of the THz waves F_- . Other parameters are the same as in Fig. 1(c,d). (c) The power spectra of F_- in (b). (d) The peak field strengths $|F_{\pm}|_{\max}$ of the THz pulses as a function of $\sin\theta$ with $\theta \in [0^\circ, 15^\circ, 30^\circ, 45^\circ, 60^\circ, 75^\circ]$.

FIG. 3 (color online). The scaling rule of the THz emission. (a) The peak field strengths $|F_{\pm}|_{\max}$ of the THz pulses as a function of the laser intensity. The plasma parameters are $n = 0.0001n_c$, $L = 50\lambda$ and the laser pulse parameters $d_L = 100\lambda$ and $\theta = 45^\circ$. (b) $|F_{\pm}|_{\max}$ of the THz pulses as a function of the electron density n . The laser pulse parameters are $a_0 = 0.5$ and $\theta = 45^\circ$. For a given plasma density n , we take $L = d_L = \lambda_p$. The dashed lines are fitted curves.

FIG. 4 (color online). 2D spatial plot of the pure THz magnetic field B_z from 2D-PIC simulation. We take $n = 0.0025n_c$, corresponding to $\lambda_p = 20\lambda$ and $\omega_p/2\pi = 14.9$ THz. The plasma length is $L = 25\lambda$. The laser pulse is s -polarized, focused on the plasma slab surface, and has parameters $a_0 = 0.5$, $w_L = 30\lambda$, $d_L = 20\lambda$ and $\theta = 50^\circ$. The dashed rectangle shows the plasma region, the solid arrow marks the laser propagation axis, and the dashed arrows the THz emission directions, one along the laser propagation and another along the specular reflection direction.

This figure "fig1.JPG" is available in "JPG" format from:

<http://arxiv.org/ps/physics/0702007v1>

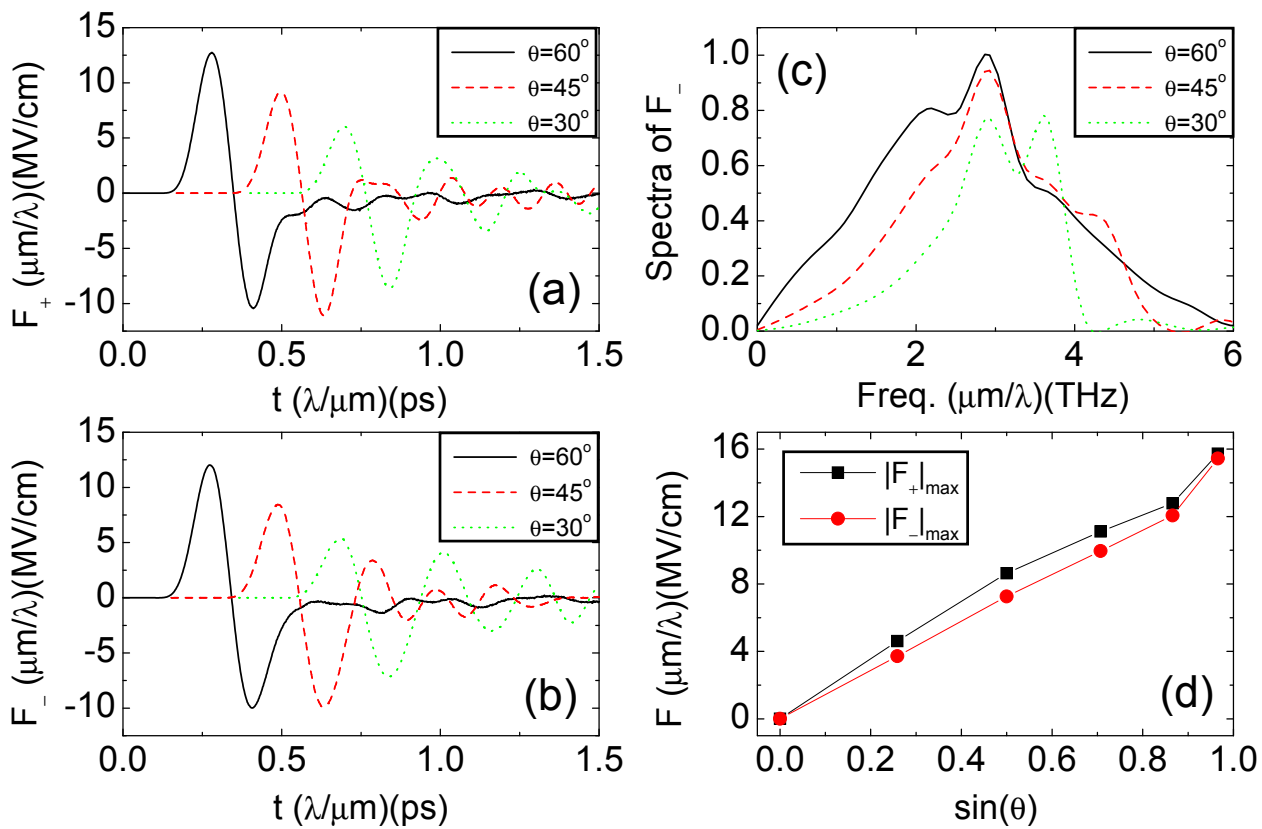


Figure 2

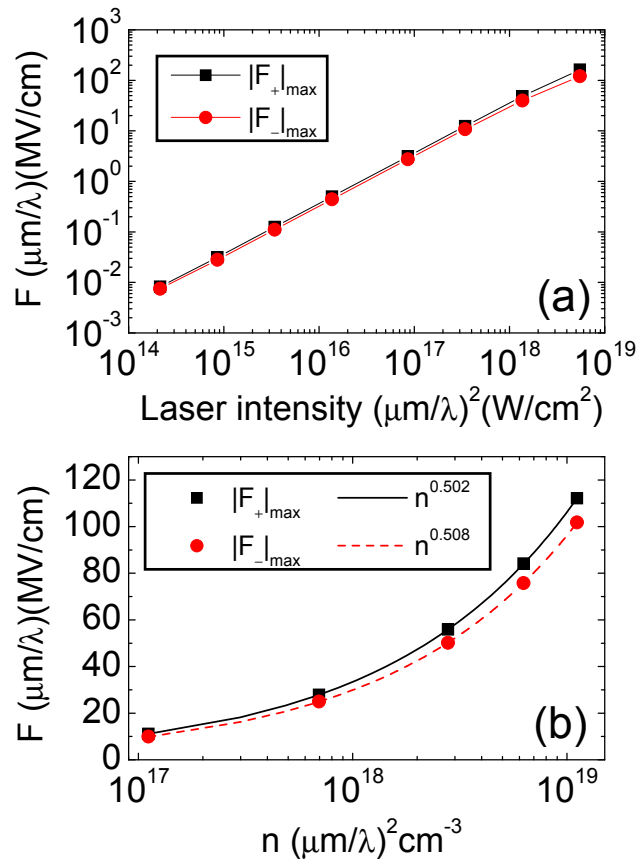


Figure 3

This figure "fig4.JPG" is available in "JPG" format from:

<http://arxiv.org/ps/physics/0702007v1>